

AD-A282 034



0

June 15, 1994

Reprint

THE SOLAR CYCLE VARIATION OF CORONAL TEMPERATURE AND DENSITY DURING CYCLE 21-22

PE 61102F  
PR 2311  
TA G3  
WU 27

M. Guhathakurta\*, R.R. Fisher\*\*, R.C. Altrock

Phillips Lab/GPSS  
29 Randolph Road  
Hanscom AFB, MA 01731-3010

DTIC  
ELECTE  
JUN 21 1994  
S B D

PL-TR-94-2163

\*Laboratory for Atmospheric and Space Physics, University of Colorado, Boulder CO \*\*Laboratory for Astronomy and Solar Physics, NASA/GSFC, Greenbelt, MD - Reprinted from Adv. Space Res. Vol. 14, No. 4 pp (4)49-(4)52, 1994

Approved for public release; distribution unlimited DTIC QUALITY INSPECTED 8

94 6 20 01 4

In this paper we characterize the temperature and the density structure of the corona utilizing co-spatial spectrophotometric observations during the descending phase of cycle 21 through the ascending phase of cycle 22. The data include ground-based intensity observations of the green (5303Å Fe XIV) and red (6374Å Fe X) coronal forbidden lines from Sacramento Peak and synoptic maps of white-light K-coronal polarized brightness,  $pB$  from the High Altitude Observatory, and photospheric magnetographs from the National Solar Observatory, Sacramento Peak. A determination of plasma temperature  $T$  can be derived unambiguously from the intensity ratio Fe X/Fe XIV, since both emission lines come from ionized states of Fe, and the ratios are only weakly dependent on density. The latitudinal variation of the temperature and the density within the descending and the ascending phases of solar cycle 21 and 22 are presented. There is a large-scale organization of the inferred coronal temperature distribution; these structures tend to persist through most of the magnetic activity cycle. This distribution differs in spatial and temporal characterization from the traditional picture of sunspot and active region evolution over the range of sunspot cycle.

94-18947

14. SUBJECT TERMS Solar corona, Solar cycle, Solar temperature			15. NUMBER OF PAGES 4
			16. PRICE CODE
17. SECURITY CLASSIFICATION OF REPORT UNCLASSIFIED	18. SECURITY CLASSIFICATION OF THIS PAGE UNCLASSIFIED	19. SECURITY CLASSIFICATION OF ABSTRACT UNCLASSIFIED	20. LIMITATION OF ABSTRACT SAR

## THE SOLAR CYCLE VARIATION OF CORONAL TEMPERATURE AND DENSITY DURING CYCLE 21-22

M. Guhathakurta,\* R. R. Fisher\*\* and R. C. Altrock\*\*\*

\* *Laboratory for Atmospheric and Space Physics, University of Colorado, Boulder, CO, U.S.A.*

\*\* *Laboratory for Astronomy and Solar Physics, NASA/GSFC, Greenbelt, MD, U.S.A.*

\*\*\* *Philips Laboratory (ASFC), Geophysics Directorate, National Solar Observatory/Sacramento Peak, Sunspot, NM, U.S.A.*

DTIC  
 ELECTE  
 JUN 21 1994  
 S B D

### ABSTRACT

In this paper we characterize the temperature and the density structure of the corona utilizing co-spatial spectrophotometric observations during the descending phase of cycle 21 through the ascending phase of cycle 22. The data include ground-based intensity observations of the green (5303Å Fe XIV) and red (6374Å Fe X) coronal forbidden lines from Sacramento Peak and synoptic maps of white-light K-coronal polarized brightness,  $pB$  from the High Altitude Observatory, and photospheric magnetographs from the National Solar Observatory, Sacramento Peak. A determination of plasma temperature  $T$  can be derived unambiguously from the intensity ratio Fe X/Fe XIV, since both emission lines come from ionized states of Fe, and the ratios are only weakly dependent on density. The latitudinal variation of the temperature and the density within the descending and the ascending phases of solar cycle 21 and 22 are presented. There is a large-scale organization of the inferred coronal temperature distribution; these structures tend to persist through most of the magnetic activity cycle. This distribution differs in spatial and temporal characterization from the traditional picture of sunspot and active region evolution over the range of sunspot cycle.

### INTRODUCTION

Knowledge of the basic physical conditions like temperature and density in the corona is fundamental to our understanding of the dominant physical processes that drives the corona and its solar-terrestrial connections via the interplanetary medium.

However very few accurate measurements have been made of the temperature of the inner corona. Recently Guhathakurta *et al.* /1/ and Guhathakurta and Altrock /2/, determined the temperature structure of the inner corona utilising co-temporal observations of the intensities of XUV, the coronal green line Fe XIV and the coronal red line Fe X during the total solar eclipse of March 1988, and estimated average temperature during the period 1984-1991 respectively. These studies provide a method for a systematic study of the latitudinal variation of the temperature and density as a function of the phase of the solar cycle.

Solar cycle variations of the density of the corona was first proposed by Allen /3/. A good representation of the coronal solar minimum with constant densities with respect to heliomagnetic latitude in the polar hole regions and an axisymmetric equatorial (neutral sheet) belt-like distribution of densities has been provided by Guhathakurta /4/,/5/. A classical representation of the maximum type corona assumes a spherical symmetry. However there is no systematic study of the average global density of the corona or the latitudinal variation of the density as a function of the phase of the solar cycle.

Variations of the coronal temperature and density as a function of latitude and phase of the solar cycle provide an important constraint necessary to model the solar wind outflow.

Daily observations of the solar corona are made at the National Solar Observatory at Sacramento Peak with the Photoelectric Coronal Photometer /6/. These observations have been made in the lines at 6374 Å and 5303 Å which are formed at approximate temperatures of 1 and 2 MK respectively in units of  $10^{-6} B_{\odot}$ , the brightness of the solar disk, at the given wavelengths /7/. The 1.1' entrance aperture is scanned daily around the limb at 1.15  $R_{\odot}$ .

Since 1980, the imaging K-coronameter Mark III (/8/) of the High Altitude Observatory at Mauna Loa Solar Observatory in Hawaii has measured the distribution of coronal polarized brightness in white-light in units of  $10^{-8} I_{\odot}$ , the brightness of the disk center, as a function of height and azimuth around the limb of the sun almost daily.

A set of synoptic observations of the longitudinal component of the photospheric magnetic field has been collected by the National Solar Observatory, and these are used in this study to provide a sense of the spatial and temporal evolution of the magnetic field of the sun during the period of this study.

### INTERPRETATION OF OBSERVED LINE PROFILES

In order to interpret the observed intensities we derive theoretical intensity profiles to be compared with the observations using the same general approach described in /1/ where we assume the following model corona: (1) Intensity variation is a function of radial distance  $r$ , along the line-of-sight, (2) collisional and radiative excitation processes, (3) ionization equilibrium distribution of ionic species, and (4) that the helium abundance  $A_{He} = 0.0851$  /3/.

#### The Intensity of Forbidden Lines of Fe XIV and Fe X

The emissivity  $E_i$ , of a forbidden line in the low corona is approximated by,

$$E_i = D_i(T)n^{\gamma}(\text{erg cm}^{-3} \text{ s}^{-1} \text{ sr}^{-1}); \quad (1)$$

where  $i=g$  for green line intensity  $I_g$ , and  $i=r$  for red line intensity  $I_r$ . Here  $D(T)$  depends on the chemical abundances and the specific transitions as well as on the electron temperature  $T$  and to some extent on the radiation field. For forbidden coronal lines primarily excited by collisions but for which the radiation field is also important  $\gamma$  has a value between 1 and 2. The intensity observed at a height  $x$  above the limb is as described below by

$$I_i(x) = R_{\odot} \int_{-\infty}^{\infty} E_i(y) dy = 2R_{\odot} \int_x^{\infty} E_i(r) \frac{r dr}{(r^2 - x^2)^{3/2}}. \quad (2)$$

Using the same approach as in /1/ we can simplify the above equation and rewrite it as

$$I_i(x) = R_{\odot} \left( \frac{2\pi h_0}{\gamma_i} \right)^{1/2} x^{3/2} E_i(x_0) \exp \left[ \frac{-\gamma_i(x - x_0)}{h_0 x x_0} \right] \quad (3)$$

where  $h_0$  is a scale-height parameter,  $n_0$  is base density and  $x_0$ , is some reference height.

#### Theoretical Emissivity of Fe XIV, Fe X

We have used Mason's /9/ excitation calculations for a dilution factor of 0.3, together with the ionization equilibrium calculations of Arnaud and Rothenflug /10/, and the abundances of Allen /3/ to calculate  $E_g$  and  $E_r$  respectively. The quantities are (/1/, /2/)

$$D_g(T) = \frac{E_g}{n^{1.66}}, \quad D_r(T) = \frac{E_r}{n^{1.66}}. \quad (4)$$

### TEMPERATURE DETERMINATION FROM EMISSION LINES

From the previous analysis we have the following equation for the intensity ratio:

$$\frac{I_r(x)}{I_g(x)} = .99 \left[ \frac{D_r(T)}{D_g(T)} \right] n(x)^{-0.02} \approx \left[ \frac{D_r(T)}{D_g(T)} \right] \quad (5)$$

Theoretical values for the ratio  $\frac{D_r}{D_g}$  is presented elsewhere /1/. We notice that a dramatic change in the intensity ratio implies a small change in temperature and therefore the precise calibration of each individual observation has minor influence on the temperature determination.

An uncertainty of one order of magnitude in the ratio of  $\frac{I_g}{I_r}$  leads to an error of only  $\pm 12\%$  in estimating temperature. Thus this method is a sensitive way of establishing temperature for the inner corona. Inspection of the above equation shows that the intensity ratio is a strongly varying function of temperature,  $T$ , but only weakly varying function of density,  $n$ . To form an approximate coronal temperature distribution we have formed the ratio  $I_g(\theta, \phi)/I_r(\theta, \phi)$  and applied equation 5. In doing this we attempt to avoid the situation of a meaningless result by retaining only those values of  $I_g$  and  $I_r$  which exceed the estimated photometric threshold of sensitivity by a factor of 5.

## CONCLUSIONS

The data sets and the estimates of the coronal temperature as inferred from the FeX/Fe XIV line ratio are shown in Figure 1. The synoptic data sets, the polarized brightness,  $pB$ , of the K-corona, the photospheric longitudinal magnetic field, the inferred distribution of temperature in the corona and the Fe X and Fe XIV emission line intensities are displayed from the top of the diagram toward the bottom. The data are arranged so as to convey both temporal and spatial information. To eliminate high frequency noise associated with rapid evolution and transient activity, we have added together data sets for two rotations to form a two-rotation average synoptic distribution for the observed quantities. These two-rotation synoptic averages are plotted adjacent to each other so that the data are given as both a function of solar latitude ( $y$ -axis) and a mixed coordinate which has both spatial and temporal information ( $x$ -axis). On the scale of a single two-rotation average, the observed quantity is displayed as a function of solar latitude and longitude, assuming a latitude invariant Carrington rotation rate. A singular solar feature persisting for several rotations is seen sequentially in this display as series of dots along the  $x$ -axis having a temporal frequency of about 6.5 visualizations per year, at the observed latitude of some given feature. The intensity scale goes in the decreasing order from white to pink to green. There are several features that become obvious when looking at this figure:

- (1) There is an organization of the large-scale coronal temperature distribution which differs from the corresponding white light density distribution. Generally, this organization takes the form of two zonal bands each about 20 degrees of solar latitude in width where the low latitude boundaries are located around 50N and 50S.
- (2) These structure tends to persist through most of the solar activity cycle. Near the maximum of the sunspot cycle the zones expand toward the solar poles.
- (3) The temperature of these zones at the reference height of  $1.15 R_{\odot}$  is about 500,000 K hotter than the mean temperature inferred for the corona near the equator of the sun.
- (4) The higher temperature material of these zones tends to lie over regions where magnetograph observations indicate a change in polarity of weak large-scale magnetic fields.
- (5) The higher temperature structures coincide with the locations of high latitude white light streamers detected at coronal altitudes of  $1.3 R_{\odot}$ .

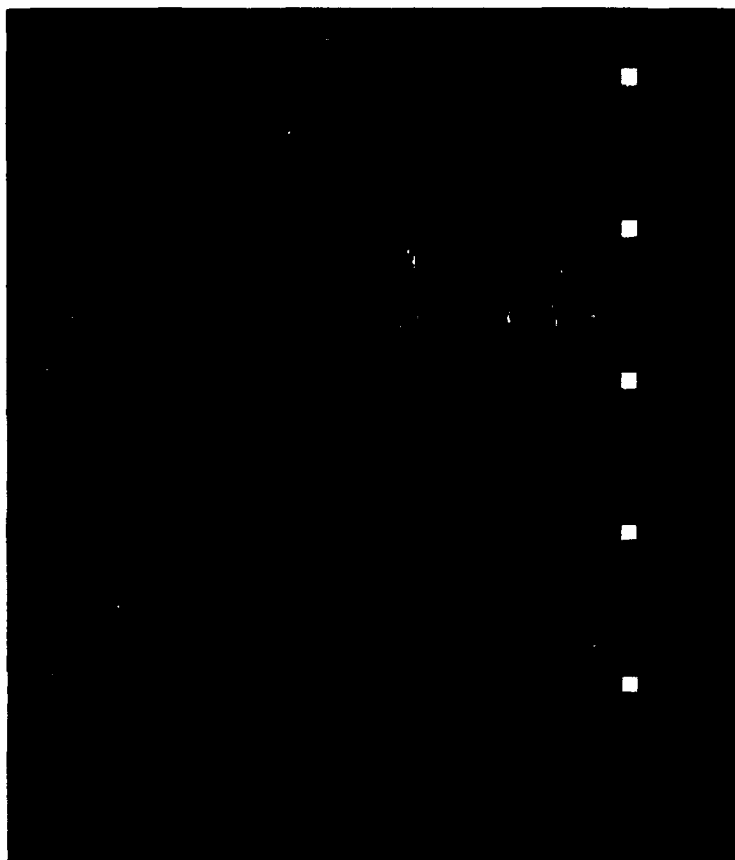
The high temperature large-scale coronal structures exhibit temporal and spatial characteristics similar to those of polar crown filaments (/11/, /12/. These regions appear to be the coronal consequence of the evolution of adjacent large-scale weak magnetic fields of opposite polarity.

## ACKNOWLEDGEMENT

This research was supported by a NASA summer faculty fellowship to one of us (M. Guhathakurta) and would like to thank all the individuals in SDAC group at GSFC for all the assistance with facilities and analysis that they provided. Observations at NSO/SP were obtained by Evans Facility observers under the supervision of Lou B. Gilliam, Chief Observer. K-coronameter data were supplied to us by D. Sime of the HAO. Some data reduction support was provided by Timothy W. Henry (NSO/SP) and Vic Tisone (NCAR/HAO). We would like to thank J.W. Harvey (NSO/KP) for providing the synoptic magnetogram data.

## REFERENCES

1. Guhathakurta, M., Rottman, G.J., Fisher, R.R., Orrall, F.Q. and R. Altrock, *Ap. J.*, April, **388**, 633, 1992.
2. Guhathakurta, M., and R. C. Altrock, *Astronomical Society of the Pacific Conference Series*, **27**, 395, 1992.
3. Allen, C.W., *Astrophysical Quantities* (3d ed., London: Athlone), 1973.
4. Guhathakurta, M., *Dissertation: The Large and Small Scale Density Structure in the Solar Corona*, University of Denver, Denver, CO, 1989.
5. Guhathakurta, M., Holzer, T.E., and MacQueen, R.M., submitted to *Ap. J.*, 1992.
6. Smartt, R.N., *Proc. SPIE*, **331**, 442, 1982.
7. Altrock, R.C., *Climate Impact of Solar Variability* Greenbelt, MD, NASA Conf. Publ. 3086, p. 287, 1990.
8. Fisher, R.R., McCabe, M., Mickey, D., Seagraves, P., and Sime, D.G., *Ap. J.*, **280**, 873, 1984.
9. Mason, H.E., *Mon. Not. R. Astr. Ser.*, **170**, 651, 1975.
10. Arnaud, M. and Rothenflug, R., *Astron. Astrophys. Supp. Ser.*, **60**, 425, 1985.
11. Guhathakurta, M. and Fisher R.R., submitted to *Ap. J. Lett.*, 1992.
12. McIntosh, P.S., *Astronomical Society of the Pacific Conference Series*, **27**, 14, 1992.



Accession For	
NTIS GRA&I	<input checked="" type="checkbox"/>
DTIC TAB	<input type="checkbox"/>
Unannounced	<input type="checkbox"/>
Justification	
By	
Distribution	
Availability Codes	
Dist	Avail and/or Special
A-1	20

Fig. 1. Evolution of solar corona as seen at (a) green line in  $10^{-6} B_{\odot}$ , (b) red line in  $10^{-6} B_{\odot}$ , (c) the temperature estimate (in MK) of the inner corona at height  $1.15 R_{\odot}$  from line ratio, (d) the photospheric magnetic field from Kitt peak, (e) and the coronal white-light from Mauna Loa Hawaii in  $10^{-8} I_{\odot}$ , for Carrington Rotations 1743-1850 for heliographic latitudes  $-90^{\circ}$  to  $90^{\circ}$ . The maxima and minima of each plot is printed in their respective unit of measurement.